Journal of Advances in Science and Technology
Vol. 22, Issue No. 2, April-2025, ISSN 2230-9659

DOI: https://doi.org/10.29070/0r50yg15

Check for updates

Assessing the Influence of Air Pollution on Atmospheric Electrical Parameters and Ecological Variability

Brijesh Kumar Vishwakarma [1] * , Dr. Ram Nihor [2]

1. Research Scholar, Shri Krishna University, Chhatarpur, M.P., India
brijesh185@gmail.com ,
2. Assistant Professor, Shri Krishna University, Chhatarpur, M.P., India

Abstract: This study investigates the correlation between air pollution levels and atmospheric electrical parameters, focusing on their ecological implications. Using real-time data from multiple monitoring stations, we analyzed variations in electric field strength, ion concentration, and air conductivity across different pollution levels. The findings indicate a significant impact of air pollution on atmospheric electricity, suggesting potential disruptions in ecological balance. These results emphasize the need for enhanced environmental monitoring and regulatory measures.

Keywords: Atmospheric electricity, air pollution, ecological impact, electric field variability, environmental monitoring

X

INTRODUCTION

Atmospheric processes, both natural and man-made, are on-going processes that shape Earth's atmosphere. Atmospheric electrical characteristics are one of these variables that significantly influences ecological systems and the state of the environment. If we want an accurate picture of Earth's health and sustainability, we need to know how these parameters change and how they relate to environmental factors like pollutants in the air. Electric field strength, lightning activity, and atmospheric electrical conductivity are all part of the set of phenomena known as atmospheric electrical parameters. Solar radiation, weather, and air composition are only a few of the many variables that might affect these values. They play an important role in driving a number of ecological processes and are also indicators of the stability and dynamics of the atmosphere.

To better understand environmental dynamics and to inform sustainable management techniques, it is crucial to study the fluctuation of various electrical parameters in the atmosphere in connection to air pollution and ecology. Air quality monitoring, ecological observations, and atmospheric measurements all work together to help scientists understand the complex web of relationships between human actions, ecosystem health, and atmospheric processes. To lessen the negative effects of environmental change, multidisciplinary teams work together to create prediction models and mitigation plans. We hope to learn more about the effects of atmospheric electrical parameter fluctuation on ecological dynamics and air quality in a variety of environments by doing this study. Our goal is to better understand the interplay between ecosystems, air pollution, and atmospheric electricity by collecting data in the field, conducting experiments in the lab, and analysing the results. We hope that our study will help in the creation of

comprehensive policies to protect the environment and improve people's lives by illuminating the processes and drivers of these linkages.

METHODOLOGY

CRYSTAL GROWTH OF PURE AND ZrO_2 ADDED $YBa_2Cu_3O_{7-s}$

It is clearly defined cation stoichiometry and straightforward synthesis, $YBa_2Cu_3O_{7\_s}$(YBCO) has shown to be the most crucial among the many high temperature superconductors for fundamental studies.

SIZE OF THE CRUCIBLE AND HEATING PROCESS

It is not required to utilise huge crucibles because the issue of controlling the nucleation, which is a more important aspect of single crystal growth, limits the size of the crystals rather than the size of the crucible.

It is important to elevate the temperature for heat treatment over the liquidus line, but not much above it due to the formation Phase.

CRYSTAL GROWTH

In a molar ratio of 1:2:3, high purity Y_2O_3 (99.99%), BaCO3 (99%), and CuO (99.99%) were employed as the starting ingredients.

Formation of $YBa_2Cu_3O_{7-}$ crystals

The melt is composed of a mixture of Y_2BaCuO_x (211) particles and Ba-Cu at the homogenization temperature. The peritectic reaction progresses slowly as the temperature drops at a rate of 2°C/hr, and the liquid has a composition that is in equilibrium with $Y_2BaCuOx$ and the $YBa_2Cu_3O_{7-\delta}$ phase with no tendency for $YBa_2Cu_3O_{7-\delta}$ crystal growth.

GROWTH OF $Bi_2Sr_2Ca_{1-x}Ce_xCu_2$ SINGLE CRYSTALS

With regards to high temperature superconductors, intriguing earths are fundamental. Since the attractive cooperation between uncommon earth particles and electrons or openings, which causes superconductivity, is commonly observed to be exceptionally powerless in the oxide framework, the presence of attractive intriguing earth particles no affects superconductivity.

$Bi_2Sr_2Ca_{1-x}Ce_xCu_2$ crystals were created using the flux approach in a gradient furnace with slow cooling. High purity mixes of Bi_2O_3, $SrCO_3$, $CaCO_3$, CeO_2 and CuO made up the initial compositions.

GLASS FORMATION

Numerous investigations have been conducted on the fabrication of high T_c superconducting materials using the glass ceramic technique since the discovery of glass formation in the Bi-Sr-Ca-Cu-0 system.

After properly wet grinding with acetone, high purity chemicals of Bi_2O_3, $SrCO_3$, $CaCO_3$ and CuO were

taken and placed in a recrystallized alumina crucible with the nominal composition $Bi_2Sr_2CaCu_2$ .The charge underwent two to three cycles of intermediate grinding while being calcined at 750°C for 15 hours.

SYNTHESIS AND EXTRACTION OF FULLERENES

Fullerene Generator

The Kratschmer-Huffman type generator is similar to the generator created for the synthesis of fullerenes. The stainless steel chamber is 25 cm long and has an inner diameter of 20 cm. The cylindrical chamber's side wall is covered with three copper electrodes that have delicate moving mechanisms. Different diameters of graphite rods can be put into the copper electrodes.

Soot production

At the tip of the copper electrodes, spectroscopic grade graphite rods of two different sizes—10 mm and 6 mm—are installed. By removing the top flange of the chamber, the graphite electrodes were repaired and replaced.

Helium gas pressure

Although fullerenes have been discovered to form in a number of inert atmospheres, including argon and molecular nitrogen, helium is now the preferred choice due to its very high fullerene yield.

Purity and size of the graphite rod

Our early research using subpar graphite rods led to fullerenes of poor quality. The use of highly pure graphite rod produced fullerenes of good quality, meaning they were free of any aromatic hydrocarbon contamination.

Arcing gap

To localise the heat produced at the ends of the graphite rod during arcing, the ends were kept in a sort of close proximity to one another such that the majority of the power was lost in the arc and not in the ohmic heating of the rod.

SOXHLET EXTRACTION

The solute that has been dissolved in a combination of solvents is sorted out during the extraction process. Depending on the situation, the solvent can either be organic or inorganic and the solute can either be in a solid or liquid media.

CHROMATOGRAPHIC SEPARATION

Chromatography is based on the principle that no separation is possible without a difference in the rates at which two substances or components migrate.

RESULT AND DISCUSSION

ELECTRICAL CONDUCTIVITY AT SKU UNIVERSITY

The number density and mobility of ions in the area are the primary determinants of the electrical conductivity of the atmosphere. Numerous elements, including aerosol particles, local climatic conditions, and the source of ionization close to the Earth's surface, affect conductivity. (Pierce, 1976; Wilkening and Romero, 1981; Retalis et al., 1991; Sheftel et al., 1994; Israelsson and Tammet, 2001; Harrison, 2003; Aplin et al., 2008; Pawar et al., 2009; De et al., 2013; Seran et al., 2017) \

DIURNAL VARIATIONS

Measured on days with good weather (apart from the monsoon season), the diurnal changes in atmospheric electric conductivity of positive and negative polarities (σ+ and σ-) were compared to the fluctuations of a few chosen meteorological factors (Nagaraja et al., 2011). The sum of the magnitudes of the positive (σ+) and negative (σ-) air conductivities over the study time was used to calculate the total air conductivity (σtotal). Figure 4-1 displays the diurnal fluctuations in air conductivity of both polarities for a typical day on March 23, 2014, throughout the summer.

Indian Standard Time (IST = UST+0530 hours) is the time scale that was employed for the investigation. Both σ+ and σ- are found to exhibit maximum in the early morning, between 0500 and 0730 hours, and then a sharp decline in conductivity levels until late afternoon, between 1300 and 1800 hours. It's intriguing to note that although σ+ and σ-variations are comparable, σ-values are somewhat greater than σ+ (Nagaraja et al., 2009). The σ- varied from $0.3x10^{-15}$ to $7.8x10^{-15}$ $\Omega^{-1}m^{-1}$ whereas σ+ varied from $0.2x10^{-15}$ to $4.9x10^{-15}$ $\Omega^{-1}m^{-1}$.

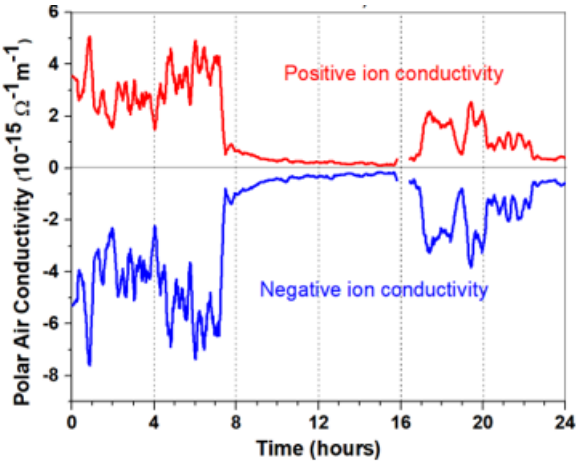

Figure 1: Diurnal variation of total air conductivity on 23-03-2014

Temperature, wind, and near-surface radioactivity are some of the variables that define the diurnal fluctuations in air conductivity close to the surface. Temperature inversion and the presence of many tiny ions are the causes of the increased air conductivity values in the early morning hours before dawn (Dhanorkar et al., 1993; Lebedyte et al., 2002; Rani et al., 2014). When the amount of radiation from the Earth's surface surpasses the amount of radiation from the sun, which usually happens at night, an

interesting phenomena known as a temperature inversion is seen close to the surface. In comparison to other seasons, wintertime had comparatively significant inversions. Pollutant particles and aerosols are trapped by this temperature inversion. It tracks gas close to the Earth's surface as well as radon gas, one of the main causes of the ionization of gas close to the surface. According to Seran et al. (2017), accumulation results in increased ionization and radon activity, which in turn produce more tiny ions that affect air conductivity. The temperature inversions are broken by solar radiation after dawn, and convection takes over. As a result, radon gas ascends by shattering the inversion layer. The air conductivity of both polarities rapidly declines after dawn as a result of vertical mixing that transports the radon gas to higher elevations.

The afternoon hours have the lowest air conductivity levels, which is caused by the least amount of radon activity close to the surface. There have been reports of similar diurnal oscillations in air conductivity measurements elsewhere (Retalis, 1991; Sasi Kumar et al., 1995), however the magnitude of σ- and σ+ varies by locale. The conductivity is greatly impacted by the weather conditions. These meteorological factors are influenced by solar radiation; changes in soil temperature, specific meteorological parameters, and overall air conductivity are examined on a typical day on March 23, 2014. Figure 2 displays the temperature fluctuation and minute averaged total air conductivity.

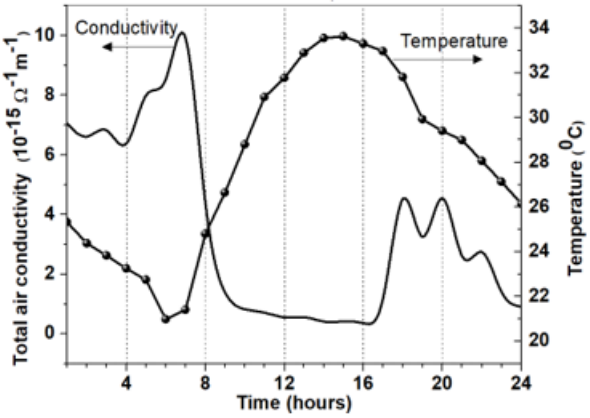

Figure 2: Diurnal variation of total air conductivity with temperature on 23-03-2014

MONTHLY VARIATIONS

The overall electrical conductivity's average daily fluctuations for each month in 2014 and 2015 are shown. By examining the mean diurnal fluctuations for each month over the observation period, it is possible to get a thorough understanding of how changes in air conductivity are influenced by meteorological conditions. Figures 4-15 to 4-18 show the mean diurnal fluctuations for 2014 and 2015.

It's noteworthy to note that, for every month, the afternoon hours had the lowest air conductivity and the early morning hours before dawn the highest. While the range of conductivity fluctuations varies from month to month in 2014 and 2015, the diurnal pattern in air conductivity levels is consistent throughout all months. It is observed that, for January, February, November and December, the total atmospheric electrical conductivity variations have reached higher values of 9 to $10x10^{-14}$ $\Omega^{-1}m^{-1}$. In contrast, during other months, the conductivity variations are relatively less.

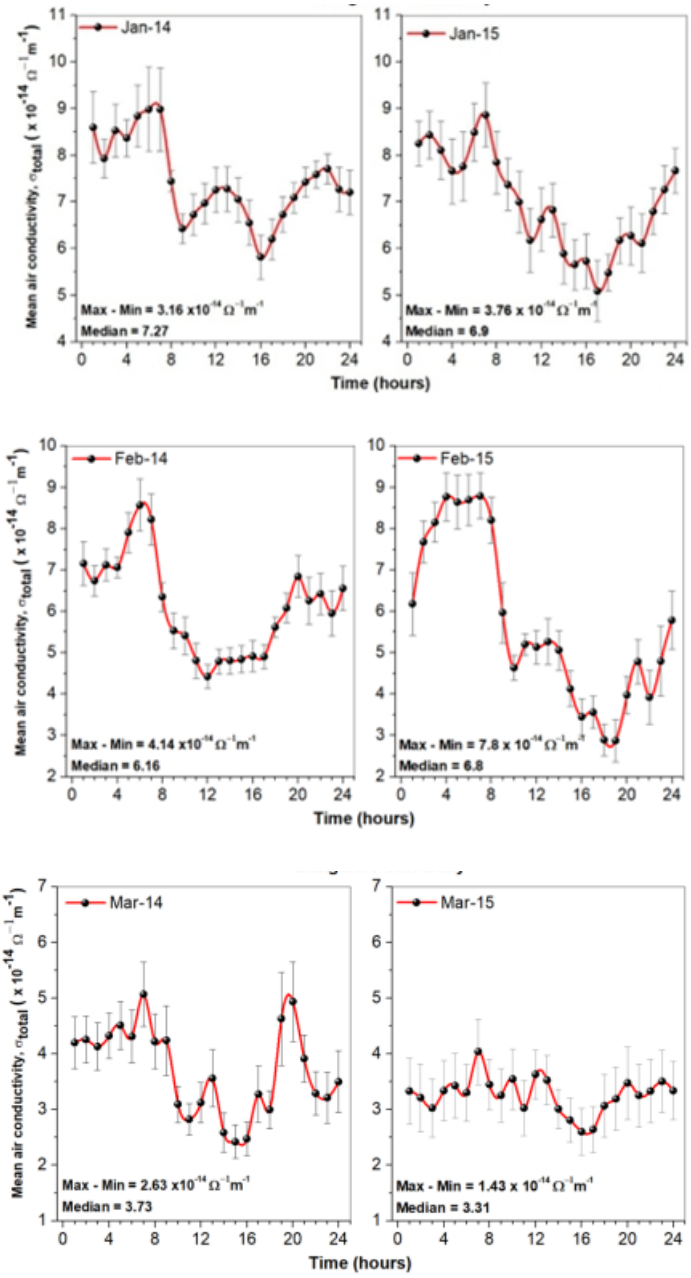

Figure 3: Averaged diurnal variations of atmospheric electrical conductivity for the months January-March for 2014 and 2015

SEASONAL VARIATIONS

At SKU University, meteorological characteristics and seasonal fluctuations in air conductivity are examined. Figure 4-25 displays the mean diurnal negative air conductivity values for each season in 2014.

Figure 4 displays the mean diurnal positive air conductivity values for each season in 2014. The winter season has the greatest positive conductivity levels, while the monsoon season has the lowest, much like the fluctuations in negative conductivity values.

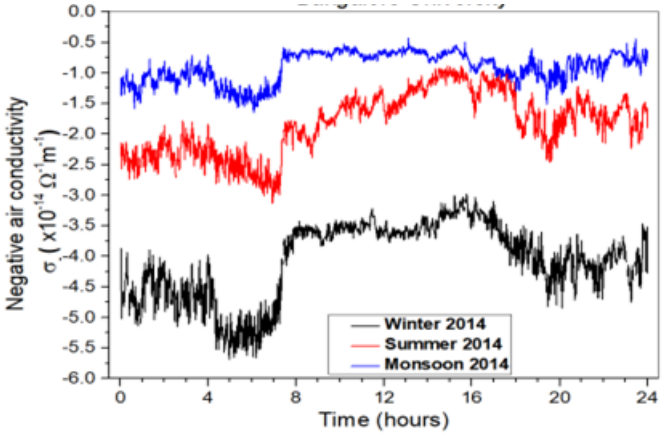

Figure 4: Diurnal variations of negative air conductivity for different seasons in 2014

RADON AND ITS PROGENIES AT NARL, GADANKI

Hoppel et al., 1986a; Nagaraja et al., 2003; Ashok et al., 2008; Amrane et al., 2013; Chandrashekara, 2017a; Karthikkumar et al., 2018; Anisimov et al., 2019; Chambers and Podstawczynska, 2019; Barbosa, 2020) are just a few of the publications that have been compiled by researchers from around the globe who are monitoring the levels of nuclear radiation and human exposure to it. Inhaling radon and its byproducts is inevitable and may lead to significant health problems, particularly in enclosed spaces. Radon gas may be released from the earth and enters the internal environment depending on the weather conditions outside. Radon, being a radioactive inert gas with a half-life of 3.823 days, ionizes the atmosphere as it disintegrates, producing 1.7x105 ion pairs/m3. These ions interact with smaller ions and air components, which contribute to the lower atmosphere's electrical properties. Variations in radon and its progeny activity mostly explain variations in the electrical conductivity of atmospheric air at the surface of the Earth (Wilkening and Romero, 1981; Prasad et al., 2005; Zhang et al., 2011; Seran et al., 2017). To learn about the health effects of radon and its derivatives, as well as its dynamics and its applications in other areas of atmospheric physics, long-term studies of outdoor radon activity and climate variables are necessary (Zahorowski et al., 2004).

DIURNAL VARIATIONS

On all days with good weather, the Radon activity recorded at NARL varies significantly during the day. There is often a dramatic drop in radon activity after dawn and a peak in the early morning hours before to sunrise. Several researchers from India and around the world have found that radon activity gradually decreases after sunrise and reaches its lowest point in the late afternoon. Just before sunset, it begins to rise again until midnight (Wilkening, 1990; Lebedyte, 2002; Nagaraja et al., 2009; Chambers et al., 2016a). Radon activity fluctuated as expected on January 15, 2013, as seen in Figure 4-32. Several dynamical mechanisms in the atmosphere combine to produce this sort of behavior. The phenomenon of temperature inversion happens when the Earth emits longwave radiation throughout the night and the temperature drops in the early morning. The process happens when the predicted behavior of temperature in the troposphere, the part of the atmosphere closest to Earth's surface, where warmer air is deposited on top of colder air, is reversed. As a result, all the gas components, aerosols, and pollution particles congregate close to Earth's

surface. Prior to dawn in the morning, radon activity is highest near the surface.

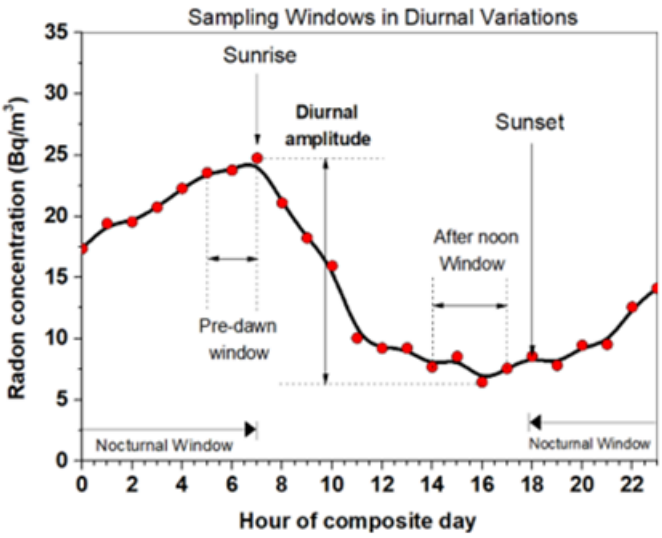

Figure 5: Activity of Radon within 24 hours window

The temperature inversion is broken after dawn when the air molecules close to the Earth's surface are heated by the sun's radiations. This drop in Radon activity after dawn is because all the suspended particles begin to ascend from Earth's surface. The vertical mixing of air parcels from the surface to higher altitudes occurs at its peak during the afternoon, when the sun's radiation progressively climbs to its maximum. During the afternoon, the concentration of radon is lower. Due to a drop in temperature, air mass building at the Earth's surface resumes after sunset and continues until dawn the next day (Desideri et al., 2006; Crawford et al., 2016). Temperature, which is mostly determined by solar radiation, plays a key influence in the diurnal changes of Radon. Radiation from the sun is responsible for the diurnal fluctuation in Radon activity. However, atmospheric physicists organize the 24-hour Radon activity cycle into several sample windows, as illustrated in Figure 4-32.

SEASONAL VARIATIONS

Radon activity at NARL varies with the seasons. According to the India Meteorological Department, the months of January through February are winter, March through May are summer, June through September is monsoon, and October through December is post-monsoon. Figure 4.50 displays the mean daily fluctuations in Radon activity for each season. Interestingly, the monsoon season had the lowest activity levels, while the winter season had the greatest activity levels, when looking at seasonal fluctuations. Monthly changes in Radon activity also exhibit this sort of behavior, and comparable findings have been reported for locations in southern India (Nagaraja et al., 2003; Prasad et al., 2005; Rani et al., 2014).

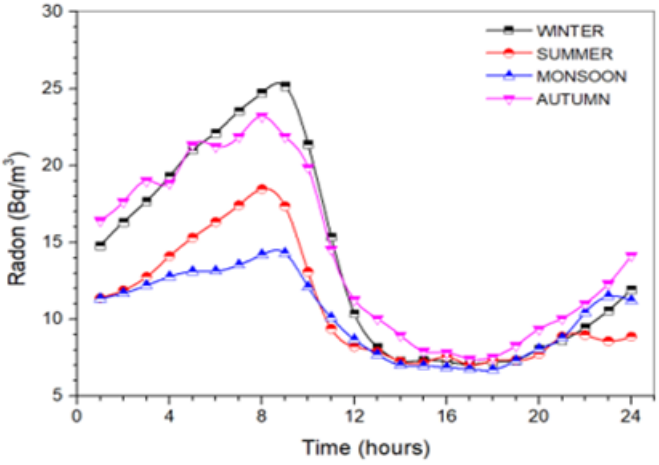

Figure 6: Averaged diurnal variations in Radon activity for individual seasons at NARL

MEMORY OF RADON ACTIVITY

Radon activity may vary greatly depending on where it comes from, which might be anything from the soil to the weather. The most noticeable variations occur on a daily, monthly, seasonal, and annual basis. Accurate information on the potential memory contained within a measured quantity's time series can only be obtained via continuous measurements. Identifying such memory, if any, is not possible in the conventional examination of time series data. Specialized methods, however, make it feasible to detect such data. The Fast Fourier Transform (FFT) is one method that examines the relationship between the observed values' amplitude and frequency. Previous work has used the fast Fourier transform (FFT) method in the frequency domain to reveal underlying periodicity in Radon, temperature, and relative humidity information. The Fourier transform method narrows the data window without taking segment averages into account. This method makes use of a consistent sampling of the necessary data to the sample.

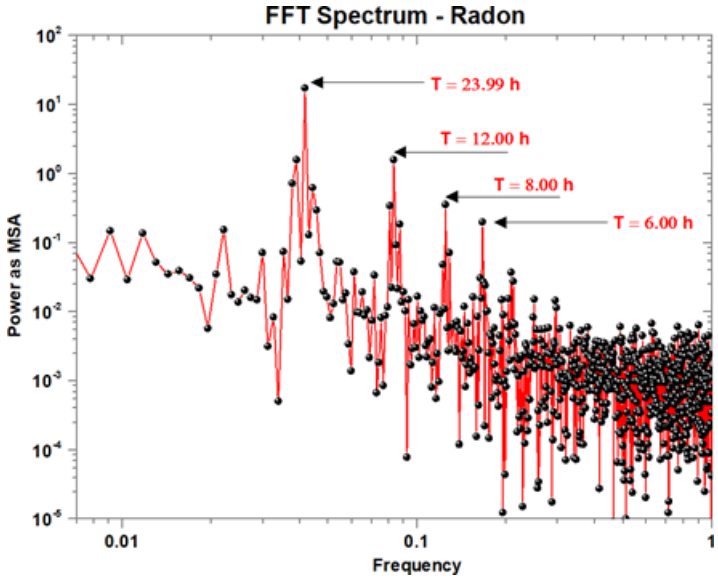

Figure 7: FFT spectra of Radon activity at NARL

CONCLUSION

Additionally, it may be possible to get knowledge on how to optimise crystal growth settings, which could improve the size and quality of synthesised crystals. Comparing the properties of the well-known high-temperature superconductors YBCO and BSCCO could shed light on their unique differences. Should the results indicate these potential directions, the study aims to investigate real-world applications, covering sophisticated electronics, energy transmission, medical imaging, scientific research, and sustainable energy solutions. The anticipated results will work together to significantly advance our knowledge of high-temperature oxide superconductors and their potential applications in numerous technical and scientific fields.

References

1. Asaoka H., Kazumata Y., Takei H. and Noda K., (1996), 'Effect of twin boundaries on flux pinning in YBa2Cu3Ox single crystals', Physica C, Vol.268, pp. 14-20.
2. Costa, F. M., Ferreira, N. M., Rasekh, S., Fernandes, A. J. S., Torres, M. A., Madre, M. A., ... & Sotelo, A. (2015). Very large superconducting currents induced by growth tailoring. Crystal Growth & Design, 15(5), 2094-2101.
3. Dragomir, M., Ma, Q., Clancy, J. P., Ataei, A., Dube, P. A., Sharma, S., ... & Gaulin, B. D. (2020). Materials preparation, single-crystal growth, and the phase diagram of the cuprate high-temperature superconductor La 1.6− x Nd 0.4 Sr x Cu O 4. Physical Review Materials, 4(11), 114801.
4. Hou, J., Yang, P. T., Liu, Z. Y., Li, J. Y., Shan, P. F., Ma, L., ... & Cheng, J. G. (2023). Emergence of high-temperature superconducting phase in the pressurized La3Ni2O7 crystals. arXiv preprint arXiv:2307.09865.
5. Huang, Y., Zhang, L., Zhou, X., Liao, L., Jin, F., Han, X., ... & Zhou, X. J. (2022). Unveiling the Degradation Mechanism of High-Temperature Superconductor Bi2Sr2CaCu2O8+δ in Water-Bearing Environments. ACS Applied Materials & Interfaces, 14(34), 39489-39496.
6. Ikram, M., Raza, A., Altaf, S., Rafi, A. A., Naz, M., Ali, S., ... & Haider, J. (2021). High Temperature Superconductors. In Transition Metal Compounds-Synthesis, Properties, and Application. IntechOpen.
7. Keimer, B., Kivelson, S. A., Norman, M. R., Uchida, S., & Zaanen, J. (2015). From quantum matter to high-temperature superconductivity in copper oxides. Nature, 518(7538), 179-186.
8. Kushwaha, S. K., Krizan, J. W., Feldman, B. E., Gyenis, A., Randeria, M. T., Xiong, J., ... & Cava, R. J. (2015). Bulk crystal growth and electronic characterization of the 3D Dirac semimetal Na3Bi. APL materials, 3(4).
9. Lei, B., Cui, J. H., Xiang, Z. J., Shang, C., Wang, N. Z., Ye, G. J., ... & Chen, X. H. (2016). Evolution of high-temperature superconductivity from a low-T c phase tuned by carrier concentration in FeSe thin flakes. Physical review letters, 116(7), 077002.

10. Mele, P., Ubaldini, A., Carnasciali, M. M., Costa, G. A., & Scavini, M. (2006). Growth and Structural Characterization of Needlelike Crystals in the Y− Ba− Cu− O System. Crystal growth & design, 6(8), 1761-1765.

11. Omar, M. A., & Fathi, S. J. (2021). The effect of partial Substitution of Lead (Pb) on the Structural and Electrical Properties of High Temperature Superconductivity System (BSCCO). ResearchJet Journal of Analysis and Inventions, 2.

12. Shams, G., & Ranjbar, M. (2019). Conductivity Fluctuation and Some Parameters of High temperature Superconductor Polycrystalline Y1Ba2Cu3O7− δ doped with Silver Nanoparticles. Brazilian Journal of Physics, 49(6), 808-819.

13. Song, Y., Bi, J., Nakamoto, Y., Shimizu, K., Liu, H., Zou, B., ... & Ma, Y. (2023). Stoichiometric Ternary Superhydride LaBeH 8 as a New Template for High-Temperature Superconductivity at 110 K under 80 GPa. Physical Review Letters, 130(26), 266001.

14. Tanaka, M., Nagao, M., Matsushita, Y., Fujioka, M., Denholme, S. J., Yamaguchi, T., ... & Takano, Y. (2014). First single crystal growth and structural analysis of superconducting layered bismuth oxyselenide; La (O, F) BiSe2. Journal of Solid State Chemistry, 219, 168-172.

15. Zhao, X.; Yu, G.; Cho, Y.; Chabot-Couture, G.; Barisic, N.; Bourges, P.; Kaneko, N.; Li, Y.; Lu, L.; Motoyama, E.M.; Vajk, O.P.; Greven, M. Crystal growth and characterization of the model high-temperature superconductor HgBa2CuO4+δ. Adv. Mater. 2006, 18, 3243.